Available online at www.sciencedirect.com
SCIENCE DIRECT
Polymer 46 (2005) 10119–10127
polymer
www.elsevier.com/locate/polymer

Preparation, characterization and mechanical properties of epoxidized soybean oil/clay nanocomposites ☆

Zengshe Liu[a,*], Sevim Z. Erhan[a], Jingyuan Xu[b]

[a] *Food and Industrial Oil Research, NCAUR, ARS, USDA, 1815 N. University Street, Peoria, IL 61604, USA*
[b] *Cereal Products and Food Science Research, NCAUR, ARS, USDA, 1815 N. University Street, Peoria, IL 61604, USA*

Received 30 December 2004; received in revised form 3 August 2005; accepted 8 August 2005
Available online 19 September 2005

Abstract

New epoxidized soybean oil (ESO)/clay nanocomposites have been prepared with triethylenetetramine (TETA) as a curing agent. The dispersion of the clay layers is investigated by X-ray diffraction (XRD) and transmission electron microscopy (TEM). XRD and TEM data reveal the intercalated structure of ESO/clay nanocomposites has been developed. The thermogravimetric analysis exhibits that the ESO/clay nanocomposites are thermally stable at temperatures lower than 180 °C, with the maximum weight loss rate after 325 °C. The glass transition temperature, T_g, about 7.5 °C measured by differential scanning calorimetry (DSC) and T_g about 20 °C measured by dynamic mechanical study have been obtained. The difference in the T_g between DSC and dynamic measurements may be caused by different heating rate. The nanocomposites with 5–10 wt% clay content possess storage modulus ranging from 2.0×10^6 to 2.70×10^6 Pa at 30 °C. The Young's modulus (E) of these materials varies from 1.20 to 3.64 MPa with clay content ranging from 0 to 10 wt%. The ratio of epoxy (ESO) to hydrogen (amino group of TETA) greatly affects dynamic and tensile mechanical properties. At higher amount of TETA, the nanocomposites exhibit stronger tensile and dynamic properties.

Keywords: Epoxidized soybean oil; Clay; Triethylenetetramine

1. Introduction

In recent years, the interest in nanoscale materials has been inspired by the fact that nanoscale materials often exhibit physical and chemical properties that are dramatically different from their bulk counterparts [1–6]. One of the most promising composite systems involves organic polymers (nylon 6) and inorganic clay minerals consisting of silicate layers [7,8]. Clay is an inexpensive natural mineral that has been used as filler for rubber and plastic for many years, but its reinforcing ability is poor so it can only be used for conventional microcomposites. A new way to improve the reinforcing ability of clay has been found. Clay can be chemically modified to make the clay complexes compatible with organic monomers and polymers. Polyamide (PA)/clay [7,9], polystyrene (PS)/clay [10], polymethylmethacrylate (PMMA)/clay [11], polypropylene (PP)/clay [12], and polyurethane (PU)/clay [13] nanocompsites have been produced in the lab and in industry in past decades. Nowadays, a lot of scientists are paying great attention to the epoxy/clay nanocomposite. This is because of fairly high polarity of the epoxy resins and curing agents which facilitates diffusion into the organophilic clay galleries and full separation of the clay layers in polymer matrix is achieved in systems [14–16].

Because of environmental concerns, the commercial utilization of biological polymers has become an active research area during past decades [17–19]. Biopolymers have potential advantages compared with synthetic petroleum polymers owing to their biodegradable properties and, in many cases, lower cost. In the United States, the major source of vegetable oil for industrial application is soybean oil. For example, United States agriculture annually produces one billion pounds of soybean oil in excess of current commercial demand. This excess capacity has resulted in lower prices for soybean oil as well as other agricultural commodities. New fields of use for these materials need to be developed and exploited. Polymer

☆ Names are necessary to report factually on available data; however, the USDA neither guarantees nor warrants the standard of the product, and the use of the name by USDA implies no approval of the products to the exclusion of other that may also be suitable.

* Corresponding author. Tel.: +1 309 681 6104; fax: +1 309 681 6340.
E-mail address: liuz@ncaur.usda.gov (Z. Liu).

0032-3861/$ - see front matter © 2005 Elsevier Ltd. All rights reserved.
doi:10.1016/j.polymer.2005.08.065

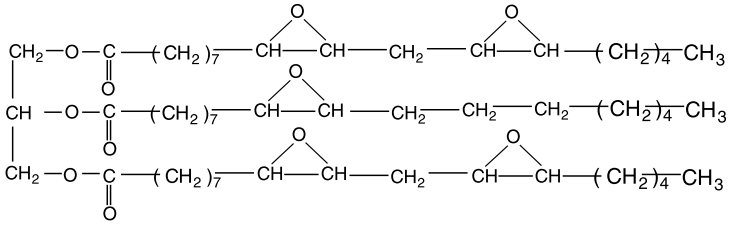

Scheme 1. Chemical structure of ESO.

scientists have shown increased interest in this field [20]. Development of economically feasible new industrial products or commercial processes from soybean oil is highly desirable. Soybean oil is mainly a mixture of triacylglycerides, which are esters of glycerol with various saturated and unsaturated fatty acids. These double bonds in unsaturated fatty acids may be converted into the more reactive oxirane moiety by reaction with peracids or peroxides. In the past, epoxidized soybean oil (ESO) has mainly been used as plasticizer for polyvinyl chloride (PVC) compounds, chlorinated rubber and polyvinyl alcohol (PVA) emulsions to improve stability and flexibility. Epoxy-containing soybean oil used as raw materials for the synthesis of new polymers suitable for liquid molding processes have been reported by Wool and co-workers [21,22]. In our previous articles [23–25], we reported preparation of epoxidized soybean oil based composites, reinforced with fibers or with combination of fiber and clay by extrusion solid freeform fabrication method. These polymeric composites demonstrate a variety of properties, ranging from elastomers to rigid plastics depending on the curing agents and comatrix. Interestingly, we have found that the polymers prepared from organophilic clay and epoxidized soybean oil show promising and valuable properties with a TETA curing agent. Recently, Kobayashi et al. [26] reported green nanocomposites developed by acid catalyzed curing of epoxidixed plant oil in the presence of organophilic clay. Mohanty et al. [27] reported the 'green' nanocomposites from cellulose acetate bioplastic and clay. Those cellulosic plastic–clay based nanocomposites demonstrate the potential for replacing and substituting polypropylene–clay nanocomosites for utilization in the automotive and transportation industries. Bio-based polymers are moving into the mainstream and polymers that are biodegradable or based on renewable resources may be competing with commodity plastics. Performance limitations and high cost, however, have limited bio-based polymers to niche markets. Nanoreinforcement of bio-based polymers with organoclay can create new value-added applications of 'green' polymers in the materials world. In this study, we focus on preparation, characterization, thermophysical and mechanical properties of these ESO/clay nanocomposites. These nanocomposites offer the potential for the diversification and application of polymers due to their excellent properties such as high heat distortion temperature, dimensional stability, improved barrier properties, flame retardancy, and enhanced physico and thermo-mechanical properties.

2. Experimental

2.1. Materials

ESO was obtained from Elf Atochem Inc. (Philadelphia, PA). Scheme 1 shows the chemical structure of ESO (oxirane contains as 7.0%). Triethylenetetramine (TETA), 60% tech, was supplied by Sigma-Aldrich Chemical Inc. (Milwaukee, WI). Scheme 2 shows the chemical structure of TETA. Cloisite 30B (montmorillonite modified with alkyl quaternary ammonium montmorillonite) was obtained from Southern Clay Products, Inc. (Gonzales, TX). All the chemicals were used without further purification.

2.2. Preparation of nanocomposites

The ESO was mixed with Cloisite 30B particles at 60 °C for 2 h using a mechanical stirrer. The mixture was sonicated at 60 °C for 2 h, followed by degassing at this temperature for a half of hour. Designated amount of curing agent, TETA, was then added to the pre-mix at room temperature. The mixture was stirred for 15 min, followed by degassing at 60 °C for 15 min. Then the mixture was poured into a container made from transparency film, and cured in an oven at 60 °C for 16 h, then at 120 °C for 48 h. The sample without clay is an amber color, semitransparent material with rubber like properties. After the introduction of clay, the samples are dark brown color, opaque materials.

2.3. Characterizations

Powder XRD analysis were performed using a Philips 1830 diffractometer operated at 40 kV, 30 mA with graphite-filtered Cu K_α ($\lambda = 0.154$ nm) radiation and a θ compensating slit. Data were acquired in $2\theta = 0.05°$, 4 s steps. The scanning range is from 2.5 to 10°. XRD was performed at room temperature.

Transition electron microscopy (TEM) specimens were cut from nanocomposites blocks using an ultramicotome

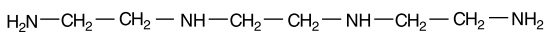

Scheme 2. Chemical structure of TETA.

(REICHERT OMU3 Ultramicrotome) equipped with a diamond knife. Transmission electron micrographs were taken with a JEOL, JEM 100C at an acceleration voltage of 100 kV.

Tensile tests were performed at 25 °C according to ASTM-D412 specification using an Instron universal testing machine (Model 1100) at a crosshead speed 50 mm/min. The dumbbell-shaped test specimen has a gauge section with a length of 33 mm, a width of 6.35 mm, and a thickness of around 4.5 mm. The dumbbell-shaped specimens were prepared by cutting the materials out of a nanocomposite plate, and five identical specimens were tested for each nanocomposite sample. Young's modulus (E) and tensile strength were obtained from the tensile tests.

The dynamic mechanical properties of the nanocomposites were obtained by using a strain-controlled Rheometric ARES Series IV rheometer (TA Instruments, Inc., New Castle, DE). Torsion rectangular geometry ($35\times12\times3$ mm) was used. The temperature was controlled by an air convection oven to within ±0.1 °C. Temperature ramp measurements were made over a range of -30 to 30 °C with small shear strain less than 0.5%. The temperature was increased by a rate of 1 °C/min. Small-amplitude oscillatory shear experiments were conducted at a frequency (ω) of 1.0 rad/s, yielding the shear storage (G') moduli and mechanical loss factor tan δ. The storage modulus represents the nondissipative component of mechanical properties. The glass transition temperature T_g of the ESO/clay nanocomposites was obtained from the peak of the loss factor curve.

DSC experiments were done on a TA Instruments (New Castle, DE) 2910 DSC-model with a computer-based controller. Typically about 10 mg of the sample was accurately weighed in an open aluminum pan and placed in the DSC module with a similar empty pan as reference. The procedure involved rapidly heating the sample to 80 °C and then holding under isothermal condition for 10 min. The system was then cooled to -50 °C at a steady rate of 10 °C/min using liquid nitrogen as the cooling medium and then holding under isothermal condition for 30 min. The system was heated to 200 °C at a steady rate of 5 °C/min. The calorimeter was calibrated with a standard indium sample.

A TA Q500 thermogravimeter was used to measure the weight loss of the ESO/clay nanocompoties under a flowing nitrogen atmosphere or air atmosphere. Generally, 20 mg of bulk nanocomposite was used in the thermogravimetric analysis. The nanocomposite samples were heated from 30 to 550 °C at a heating rate of 10 °C/min. and the weight loss was recorded as a function of temperature.

3. Results and discussion

3.1. Characterizations of ESO/clay nanocomposites

The X-ray diffraction patterns of the nanocomposites and the clay particle are shown in Fig. 1. The Cloisite 30B clay has a sharp peak at 4.5°. The peak corresponds to the [001] basal reflection of the organoclay. For the composites with 0.0, 5.0, 8.0, and 10.0 wt% clay contents, no clear peaks were observed, suggesting that silicate layers of organoclay may be exfoliated in the polymer matrix. Although it is common practice to classify a nanocomposite as fully exfoliated from the absence of (001) reflection, it is difficult to reach a definitive conclusion about the defined structure from the XRD alone. Thus, TEM techniques are necessary to characterize the composites. Fig. 2 shows TEM micrographs of ESO/clay nanocomposites containing 5.0, 8.0 and 10.0 wt% clay content, respectively. The dark lines in the figure correspond to the silicate nanolayers. TEM micrograph shows that there was no aggregation of organoclay particles. This suggests that the organophilic clay particles are well dispersed in ESO matrix. Layer spacing of the clay in the nanocomposites increased, compared to the organoclay galleries about 2 nm. There was a distribution in basal spacings. A wide distribution in basal spacings may cause the absence of (001) reflection. At this condition, it is clear that an intercalated structure of the composites was developed. Preparation of an exfoliated structure of the composites by changing process conditions will be examined and discussed in our future report.

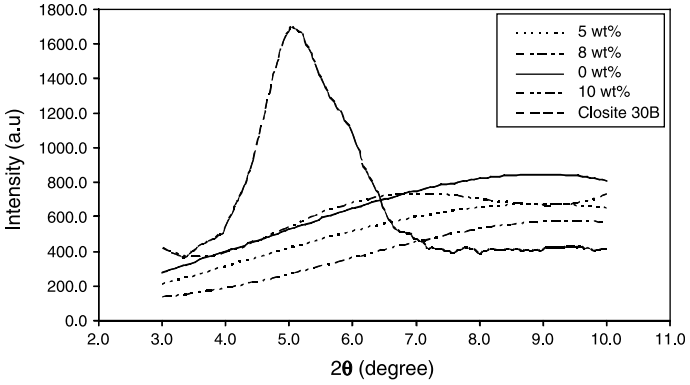

Fig. 1. X-ray diffraction of ESO/clay nanocompsoite samples.

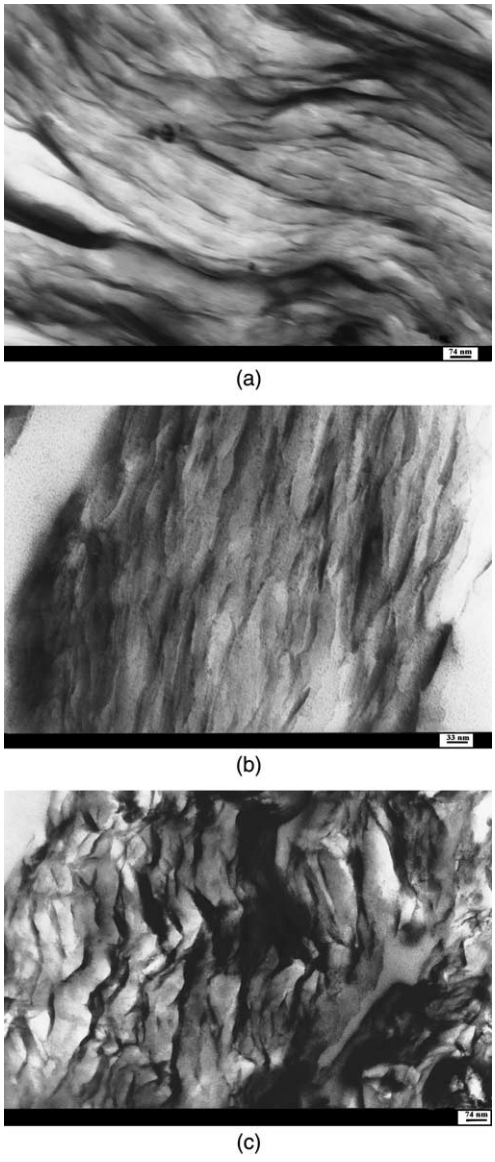

Fig. 2. TEM micrographs of ESO/clay nanocomposites containing (a) 5.0 wt%, (b) 8.0 wt% and (c) 10.0 wt% clay content.

3.2. Dynamic mechanical behavior

Fig. 3 shows the dynamic mechanical spectra (dynamic storage modulus G', and loss factor tan δ) as a function of temperature for ESO/clay nanocomposites with different clay loading. Some values of G' at various temperatures and T_g are presented in Table 1. The storage moduli initially remain almost constant at low temperatures between -30 and -10 °C for all clay loading samples (Fig. 3). The storage modulus of ESO/clay nanocomposites with 8 wt% clay content shows a slightly higher value than other samples. As temperature increases to 0 °C, the nanocomposite with 0 wt% clay content shows lower storage modulus, which is 1.54×10^8 Pa, than nanocomposites with 5 wt% clay content, which is 2.76×10^8 Pa. The nanocomposites with 8 wt% clay content shows the highest value of 4.15×10^8 Pa.

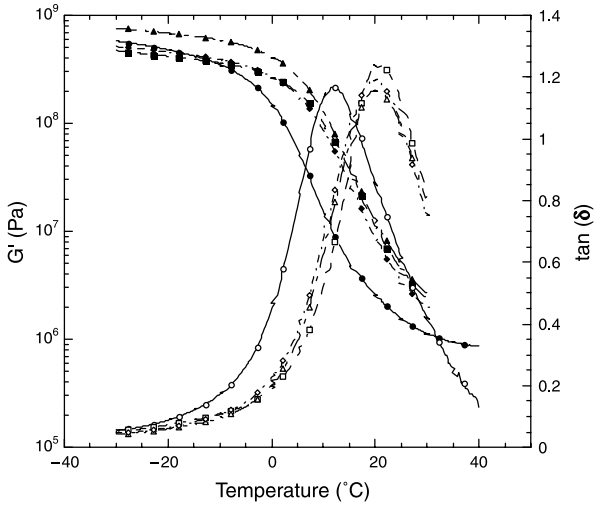

Fig. 3. Temperature dependence of the storage modulus and loss factor for the ESO/clay nanocomposites prepared by varying the clay content. Filled symbols G', opened symbols tan (δ); circle, 0.0 wt% clay; square, 5.0 wt% clay;triangle, 8.0 wt% clay; and diamond, 10.0 wt% clay [ratio of (epoxy group of ESO)/(hydrogen of the amino group), 1:1.37].

As the temperature increases further, the storage moduli of all samples exhibit drop, but sample with 0 wt% clay loading drops sharply. Then this sample shows a modulus plateau after temperature of 25 °C, where the materials behaves like a rubber. Apparently, the modulus drop corresponds to onset of segment mobility in the crosslinked polymer networks. The above results show clearly that the addition of clay up to 8 wt% into ESO matrix results in a remarkable increase of stiffness. Increasing of clay content to 10 wt% of clay shows the decreasing of storage modulus.

The glass transition temperature T_g of the ESO/clay nanocomposite was obtained from the peak of the loss factor curve. It can be seen from Table 1 that the material with 0 wt% clay content shows lower T_g, which is 11.8 °C, the nanocomposite with 5 wt% clay content is 20.7 °C. As the clay loading increases, the resulting nanocomposites show no significant difference in the glass transition temperature.

Fig. 4 gives the temperature dependence of the storage moduli and the loss factors for the ESO/clay nanocomposites prepared by varying amount of TETA. The clay content is kept constant with 8 wt%. Some values of G' at various temperatures and T_g are presented in Table 2. When the expoxy (ESO) to hydrogen (amino group) ratio of 1 to 1 is used, the resulting nanocomposite shows lower modulus,

Table 1
Dynamic storage moduli of the ESO/clay nanocomposites at various temperatures

Cloisite 30B (wt%)	Storage modulus, G' ($\times10^8$ Pa)				T_g (°C)
	−30 °C	0 °C	10 °C	30 °C	
0	5.90	1.54	0.16	0.011	11.8
5	5.00	2.76	1.08	0.025	20.7
8	7.63	4.15	1.28	0.027	19.4
10	5.20	2.75	0.88	0.020	20.2

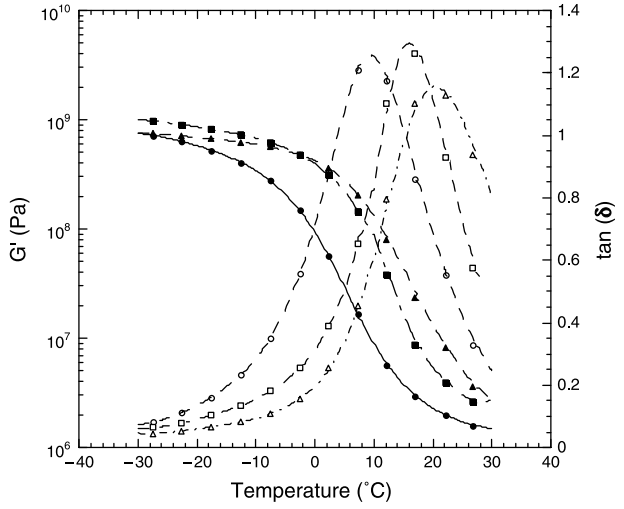

Fig. 4. Temperature dependence of the storage modulus and loss factor for the ESO/clay nanocomposites prepared by varying the TETA concentration (clay content, 8.0 wt%). Filled symbols G', opened symbols tan (δ); circle, [1:1 of (epoxy group of ESO)/(hydrogen of the amino group)]; square, [1:1.24 of (epoxy group of ESO)/(hydrogen of the amino group)]; triangle, [1:1.37 of (epoxy group of ESO)/(hydrogen of the amino group)]. Clay content, 8.0 wt%.

especially at high temperatures. An increase in the TETA concentration greatly affects the high temperature storage modulus and loss factor. Such behavior is expected, because increasing the TETA concentration increases the cross-linking density of the material. The ratio of epoxy/hydrogen of amine group in TETA is the key factor controlling the properties of the material in this case. Xu et al. [28] studied the control the viscoelastic properties of ESO-based biomaterials and found that a larger ratio of epoxy (ESO)/hydrogen (TETA) made the chemical reaction between the hydrogen on the amino group of TETA and the epoxy group on the ESO more efficient. The glass transition temperature (T_g) of formed material will be higher with larger ratio of epoxy/hydrogen than with smaller ratio. It is also possible for the amine function group to perform other reactions, for example, the amidation reaction of triacylglyceride. This would cause a displacement of stoichiometry, which could explain the decrease of T_g in the epoxy/hydrogen ratio of 1 to 1. The amidation reaction of triacylglyceride with diamine compounds needs to be further studied.

Table 2
Dynamic storage moduli of the ESO/clay nanocomposites prepared by varying epoxy/H ratio

Epoxy/H ratio	Cloisite 30B (wt%)	Storage modulus, G' ($\times 10^8$ Pa)				T_g (°C)
		30 °C	0 °C	10 °C	30 °C	
1:1	8	7.54	0.95	0.09	0.015	9.7
1:1.24	8	10.1	3.92	0.80	0.025	17.4
1:1.37	8	7.63	4.15	1.28	0.027	19.4

Table 3
Tensile mechanical properties of the ESO/clay nanocomposites with different clay content (epoxy/H ratio, 1:1.37)

Cloisite 30B (wt%)	Tensile strength (MPa)	Young's modulus (E) (MPa)	Percent elongation (%)
0	1.27	1.20	127
5	2.98	2.61	133
8	4.54	3.64	151
10	4.34	3.54	148

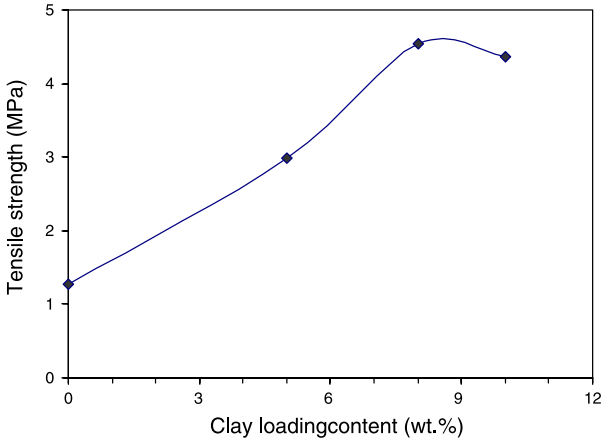

Fig. 5. Effect of clay content on tensile strength of ESO/clay nanocomposites.

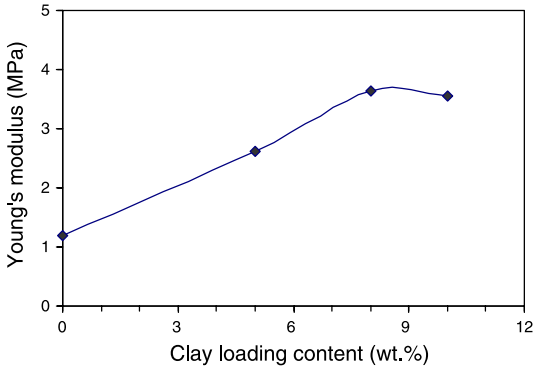

Fig. 6. Effect of clay content on Young's modulus of ESO/clay nanocomposites.

3.3. Tensile mechanical properties

The effects of the clay content on tensile properties of the ESO/clay nanocomposites are presented in Table 3. The ratio

Table 4
Tensile mechanical properties of the ESO/clay nanocomposites prepared by varying epoxy/H ratio

Epoxy/H ratio	Cloisite 30B (wt%)	Tensile strength (MPa)	Young's modulus (E) (MPa)	Percent elongation (%)
1:1	8	1.03	2.28	53
1:1.24	8	2.61	3.27	95
1:1.37	8	4.54	3.64	151

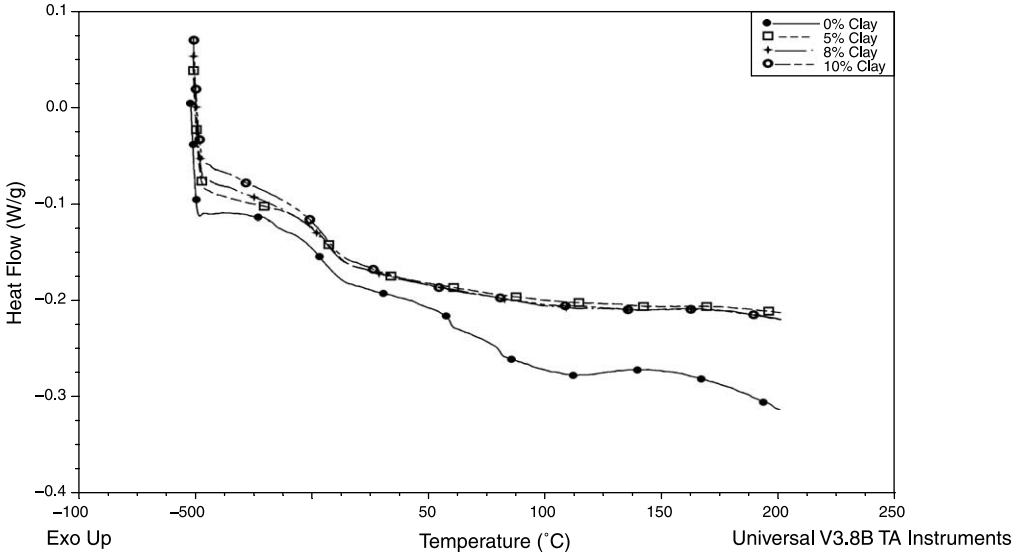

Fig. 7. DSC measurements of ESO/clay nanocomposites prepared by varying the clay content.

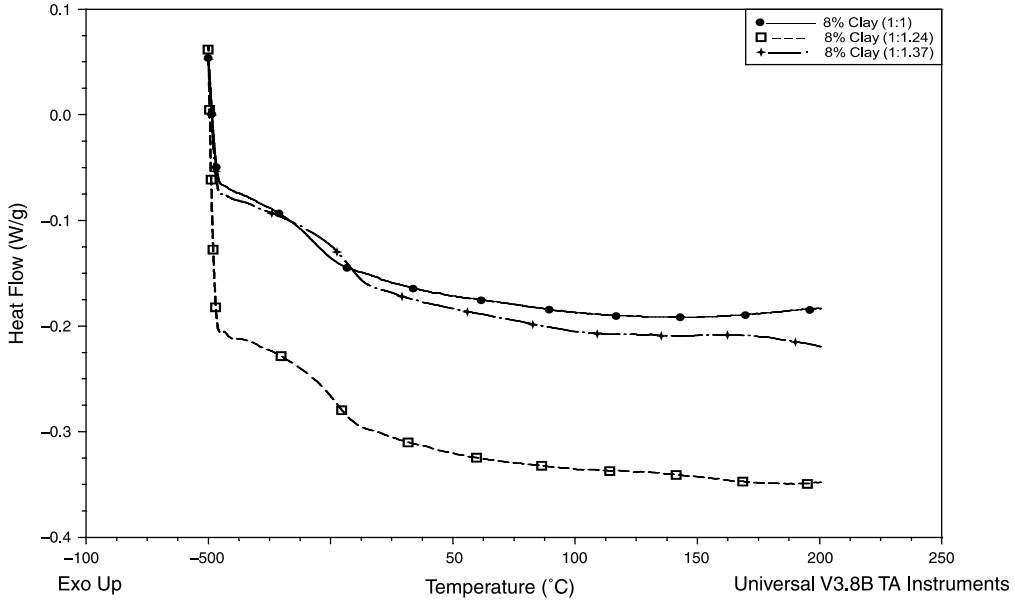

Fig. 8. DSC measurements of ESO/clay nanocomposite prepared by varying the TETA concentration.

of epoxy to hydrogen is 1 to 1.37. It can be seen that the tensile mechanical behavior of the nanocomposites highly depends upon the clay concentration. Using the data entries in Table 3, the trend of clay content influences on tensile strength and Young's modulus of the nanocomposites are clearly seen in Figs. 5 and 6. The tensile strength of nanocomposites increases rapidly from 1.27 to 4.54 MPa with increasing clay content from 0 to 8 wt%. Similarly, the modulus increases rapidly from 1.20 to 3.64 MPa with increasing clay content from 0 to 8 wt%. Slightly decrease in Young's modulus is observed when the clay content increases beyond 8–10 wt%. The similar results were reported by Liu et al. in the polypropylene/clay nanocomposites prepared by grafting-melt compounding method [29]. The nanometric dispersion of silicate layers in matrix leads to improved modulus and strength. The stiffness of the silicate

Table 5
The glass transition temperatures of ESO/clay nanocomposites prepared by varying the epoxy to hydrogen ratio (clay content, 8.0 wt%)

Epoxy/H ratio	1:1	1:1.24	1:1.37
T_g (°C)	−6.8	2.7	7.5

Table 6
The glass transition temperatures of ESO/clay nanocomposites with different clay content (epoxy/H ratio, 1:1.37)

Clay loading (wt%)	0	5	8	10
T_g (°C)	5.8	7.6	7.5	7.3

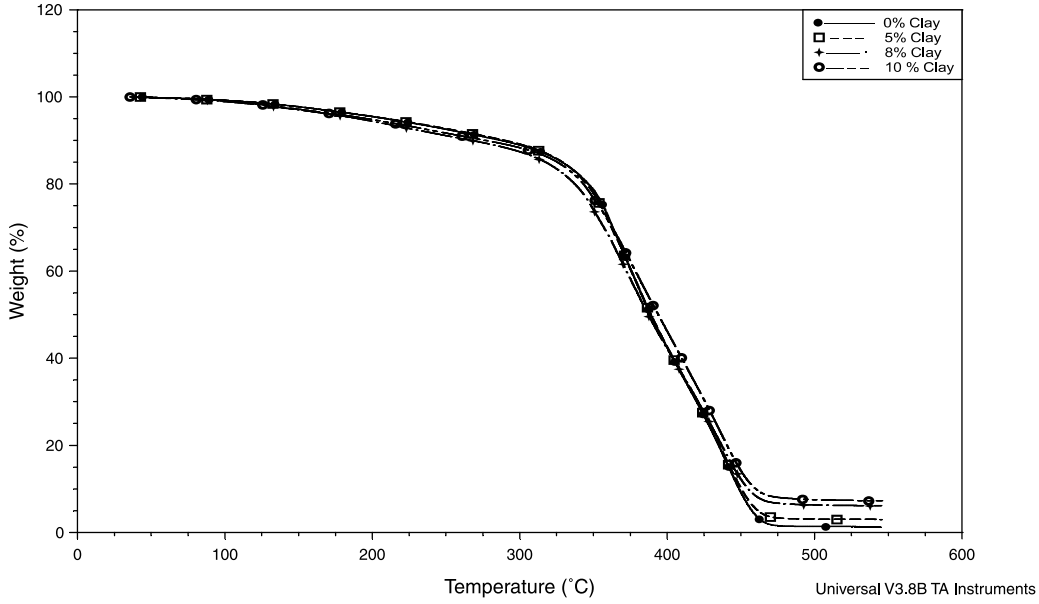

Fig. 9. TGA thermograms of weight loss versus temperature (under N_2 atmosphere).

layers contributes to the presence of immobilized or partially immobilized polymer phases. It is also possible that silicate layer orientation as well as molecular orientation contribute to the observed reinforcement effects. The lower values of tensile strength and Young's modulus above 8 wt% clay content can be attributed to the inevitable aggregation of the layers in high clay content.

As discussed earlier, the degree of crosslinking affects the dynamic properties of nanocomposites. The tensile properties of the nanocomposites prepared by varying the epoxy group to hydrogen ratio are studied and presented in Table 4. The clay content remains constant at 8 wt%. It can be seen that tensile strength and Young's modulus increases with increasing amount of TETA, in other words, decreasing the epoxy/hydrogen ratio. The tensile strength changes from 1.03 to 4.54 MPa, when the epoxy to hydrogen ratio changes from 1:1 to 1:1.37. Similarly, the Young's modulus changes from 2.68 to 3.64 MPa, This apparent increase may be contributed to the formation of higher crosslinking density of polymeric matrix due to increasing TETA amount.

The glass transition temperatures of ESO/clay nanocomposites prepared by varying the epoxy to hydrogen ratio and by varying clay content are measured by DSC. Fig. 7 and Fig. 8 show DSC curves. The glass transition temperatures (T_gs) obtained by analyzing these curves are summarized in Table 5 and Table 6. It can be seen from Table 5 that glass transition temperature, T_g, increases with decreasing the epoxy to hydrogen ratio from 1:1 to 1:1.37. The T_g changes from −6.8 to 7.5 °C. This apparent increase may be contributed to the formation of higher crosslinking density of polymeric matrix due to increasing curing agent amount. The free volume out of the gallery is reduced, and the segmental mobility within polymer out of the gallery decreased. Thus, the T_g with larger amount of the crosslinking agent will be higher. Here again it is also possible that not all amine function could react with the network, this would cause a displacement of stoichiometry, which could explain the decrease of T_g in the epoxy to hydrogen ratio of 1 to 1. However, this explanation should be validated by a further study.

Table 6 shows that an increase in T_g of nanocomposite with 5 wt% clay content is observed in comparison with polymer of 0 wt% clay content. The T_g changes from 5.8 to 7.6 °C, probably because of the restricted mobility of the chains due to the presence of organophilic clay layers between than chains of polymer. But there is no significant difference when the clay content is increases to 8 or 10 wt%. The T_gs obtained from DSC and from dynamic experiments have been compared and found that their trends are the same, but values are different. This may be due to the different heating rate employed in the experiments.

3.4. Thermogravimetric analysis

Fig. 9 shows the thermogravimetric analysis (TGA) curves of the ESO/clay nanocomposites. From the characteristic temperatures in TGA curves (Table 7), it can be seen

Table 7
TGA results of weight loss for ESO/clay nanocompsites with different clay content (under N_2)

Cloisite 30B (wt%)	Weight loss (wt%)			
	0–180 (°C)	200–300 (°C)	400–450 (°C)	500–550 (°C)
0	<1	~10	55–90	98
5	<1	~10	50–75	95
8	<1	~10	45–75	92
10	<1	~10	45–70	90

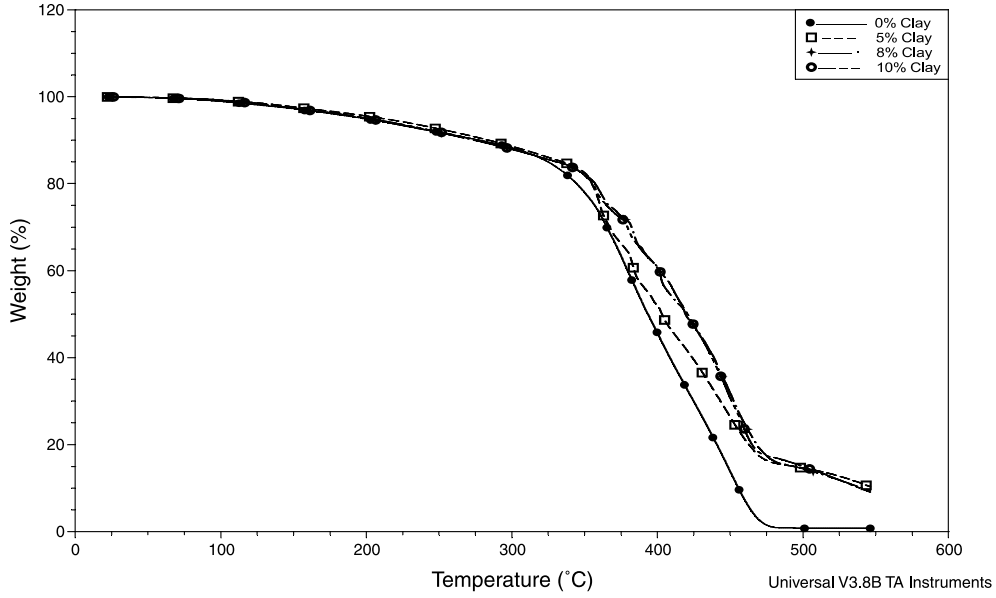

Fig. 10. TGA thermograms of weight loss versus temperature (under air atmosphere).

that the ESO/clay nanocomposites appear to be thermally stable at temperatures lower than 180 °C. These materials lose about 10% of their weight at temperature between 200 and 300 °C, followed by an abrupt weight loss after 325 °C. An 80% weight loss is observed at 440 °C. There is no significant difference between 0 wt% clay content sample and samples with clay content up to 10 wt% under N_2 atmosphere. It is important to note that the thermal decomposition experiments taken in nitrogen not in air. It is well know that for exfoliated nanocomposites, the silicate layers of clay disperse well in the polymer matrices and these well dispersed clay layers act as barriers to prevent oxidation when heated in air. If the silicate layers were not dispersed well in the polymer matrices, the intercalated nanocomposites would show relatively poor thermal properties. The thermal decomposition behaviors of polystyrene/clay and polyepichlorohydrin/clay system reported by Kim et al. [30] and Qutubuddin et al. [31] showed that the nanoscale clay layers could reduce the permeability for oxygen or volatile degradation products and improve the thermal degradation properties of nanocomposites. Fig.10 shows the thermal decomposition behavior of ESO/clay nanocomposites under air atmosphere. We have found that the material without clay clearly shows larger weight loss after 350 °C. The onset of thermal degradation temperature of nanocomposites shifted toward higher temperatures, which confirms the enhancement of thermal stability of the ESO/clay nanocomposites.

4. Conclusion

The new nanocomposite materials have been prepared from ESO and clay with TETA curing agent. A complete characterization has been carried out on these ESO/clay nanocomposites. Complementary observations through X-ray diffraction and TEM micrograph enable to give insight into the filler state of dispersion. The organophilic clay is well dispersed in the matrix. An intercalated structure of the composite is developed. Dynamic mechanical study shows the ESO/clay nanocomposites with 5–10 wt% clay content possess storage modulus ranging from 2.0×10^6 to 2.70×10^6 Pa at 30 °C. The T_g, about 7.5 °C measured by DSC and T_g, about 20 °C measured from dynamic mechanical study have been obtained. The difference of T_g between DSC and dynamic measurements may be caused by different heating rate. Clay content does not affect glass transition temperatures of nanocompsites. However, the ratio of epoxy to hydrogen in amino group greatly affects dynamic and tensile mechanical properties. The new ESO/clay nanocomposites appear to be thermally stable at temperatures lower than 180 °C. The maximum weight loss rate is observed after 325 °C. Kobayashi et al. [32] reported that the good biodegradability of the cured polymer from ESO was preliminarily found. Thus, the present nanocomposites are highly expected to be a new class of biodegradable plastics, insulation materials and coating materials from inexpensive renewable resources, contributing to global sustainability. These materials may show promise as alternative to petrochemical polymers.

Acknowledgements

The authors would like to thank Mr Gary Gross for XRD, Mr Robert Caughey for TEM and Mr A.J. Thomas for technical assistance. We would also like to thank Dr Doug Hunter of Southern Clay Products, Inc. for clay sample.

References

[1] Okada A, Usuki A. Mater Sci Eng 1995;C3:109–15.
[2] Novak BM. Adv Mater 1993;5(6):422–33.
[3] Giannelis EP. Adv Mater 1996;8:29–34.
[4] Wang Z, Pinnavaia TJ. Chem Mater 1998;10:1820–6.
[5] Shi HZ, Lan T, Pinnavaia TJ. Chem Mater 1996;8:1584–7.
[6] Lan T, Kaviratna PD, Pinnavaia TJ. Chem Mater 1995;7:2144–50.
[7] Usuki A, Kawasumi M, Kojima Y, Fukushima Y, Okada A, Kurauchi T, et al. J Mater Res 1993;8(5):1179–84.
[8] Kojima Y, Usuki A, Kawasumi M, Okada A, Fukushima Y, Kurauchi T, et al. J Mater Res 1993;8(5):1185–9.
[9] Kojima Y, Usuki A, Kawasumi M, Kamigaito O. J Polym Sci, Part A: Polym Chem 1993;31(7):1755–8.
[10] Vaia RA, Giannelis EP. Macromolecules 1997;30(25):8000–9.
[11] Lee DC, Jang LW. J Appl Polym Sci 1996;61(7):1117–22.
[12] Usuki A, Kato M, Okada A, Kurauchi T. J Appl Polym Sci 1997; 63(1):137–9.
[13] Chen TK, Tien YI, Wei KH. J Polym Sci, Part A: Polym Chem 1999; 37(13):2225–33.
[14] Kornmann X, Lindberg H, Berglund LA. Polymer 2001;42(4): 1303–10.
[15] Xu WB, Bao SP, He PS. J Appl Polym Sci 2002;84(4):842–9.
[16] Kim JK, Hu CG, Woo RSC, Sham ML. Compos Sci Technol 2005;65: 805–13.
[17] Mishra DP, Mahanwar PA. Advances in bioplastic materials. Pop Plast Packag 2000;45(7):68–76.
[18] Schroeter J. Biodegradable plastic materials. Kunststoffe 2000;90(1): 64–6 [see also p. 68–70].
[19] Fomin VA, Guzeev VV. Biodegradable polymers: status and prospects. Plast Massy 2001;2:42–8.
[20] Wool RP. Development of affordable soy-based plastics, resins, and adhesives. Chemtech 1999;29(6):44–8.
[21] Wool RP, Kusefoglu SK, Khot SN, Zhao R, Palmese G, Boyd A, et al. Affordable composites from renewable sources (ACRES). Polym Prepr (Am Chem Soc, Div Polym Chem) 1998;39:90.
[22] Wool RP, Kusefoglu SH, Zhao R, Palmese G, Boyd A, Fisher C, et al. Affordable composites from renewable sources (ACRES). 216th ACS national meeting, Boston, August 23–27 1998.
[23] Liu ZS, Erhan SZ, Xu J, Calvert PD. J Appl Polym Sci 2002;85(10): 2100–7.
[24] Liu ZS, Erhan SZ, Calvert PD. J Appl Polym Sci 2004;93(1):356–63.
[25] Liu ZS, Erhan SZ, Calvert PD. J Am Oil Chem Soc 2004;81(6): 605–10.
[26] Uyama H, Kuwabara M, Tsujimoto T, Nakano M, Usuki A, Kobayashi S. Chem Mater 2003;15(13):2492–4.
[27] Park HM, Misra M, Drzal LT, Mohanty AK. Biomacromolecules 2004;5(6):2281–8.
[28] Xu J, Liu ZS, Erhan SZ, Carriere CJ. J Am Oil Chem Soc 2004;81(8): 813–6.
[29] Liu XH, Wu QJ. Polymer 2001;42:10013–9.
[30] Kim SK, Kim JK, Chin IJ, Choi HJ. J Appl Polym Sci 2002;86: 3735–9.
[31] Qutubuddin S, Fu X. Polymer 2001;42:807–13.
[32] Tsujimoto T, Uyama H, Kobayashi S. Polym Prepr Jpn 2002;51:3811.